

HFFB technique and its validation studies

Jiming Xie^{*1} and Jason Garber²

¹Zhejiang University, Hangzhou, Zhejiang, China

²RWDI Inc., 650 Woodlawn Road West, Guelph, Ontario, N1K 1B8, Canada

(Received January 11, 2010, Revised December 2, 2010, Accepted October 3, 2013)

Abstract. The high-frequency force-balance (HFFB) technique and its subsequent improvements are reviewed in this paper, including a discussion about nonlinear mode shape corrections, multi-force balance measurements, and using HFFB model to identify aeroelastic parameters. To apply the HFFB technique in engineering practice, various validation studies have been conducted. This paper presents the results from an analytical validation study for a simple building with nonlinear mode shapes, three experimental validation studies for more complicated buildings, and a field measurement comparison for a super-tall building in Hong Kong. The results of these validations confirm that the improved HFFB technique is generally adequate for engineering applications. Some technical limitations of HFFB are also discussed in this paper, especially for higher-order mode response that could be considerable for super tall buildings.

Keywords: wind tunnel validations; high-frequency force-balance model; high-frequency pressure integration model; multi-force balance system; HFFB/aeroelastic hybrid model; field measurement; wind tunnel tests; nonlinear mode shapes; aeroelastic effects

1. Introduction

The High-Frequency Force Balance (HFFB) method provides a convenient approach in wind tunnel testing for determining wind-induced response of tall buildings. HFFB is also referred to as High-Frequency Base Balance (HFBB) in some literature because most of its applications are with the force balance being set at the model base. Since its original development about 25 years ago (Tschanz 1982), the HFFB method has been improved significantly to deal with more complex structures. While the original HFFB stands on an explicit mathematic foundation and assumptions, the improved HFFB and its extended applications require additional or alternative assumptions. The validations of the current HFFB studies are therefore important.

HFFB is basically a method that combines experimental and analytical approaches. In a mathematical model that describes the wind-induced structural response, only the wind excitation part is unknown while the structural dynamic part can be determined analytically using available structural analysis tools, such as the finite-element method. The extent of wind excitations is sensitive to the local wind environment, the building geometry, the aerodynamic interactions with adjacent structures and potentially the structural motions. The latter are called aeroelastic effects. Due to these complicated factors, the wind excitations are difficult to determine analytically. For

*Corresponding author, Professor, E-mail: jiming.xie@zju.edu.cn

most buildings, the aeroelastic effects are less significant because the building deflections are normally very small compared with the building horizontal dimensions and the building mass is often very high. With aeroelastic effects being neglected, the wind excitation can be determined through measurements on a rigid model (i.e., a HFFB model) in a simulated wind environment with modeled surroundings. The measurements consist of mean wind loads and background dynamic loads. By including these loads in the modal analysis with random-vibration equations, the structural resonance response can be calculated and the total wind loads are thus determined.

1.1 Consideration of non-linear mode shapes

In the original HFFB method, one of the main assumptions is that the building sway mode shape has to be linear, so that the generalized wind loads used in the equation of motion can be directly obtained from the measurement of the overturning moment on the tested model.

$$\tilde{P}(t) = \int_h p(z,t) \left(\frac{z}{h} \right) dz = \frac{1}{h} \int_h p(z,t) z dz = \frac{M_B}{h} \quad (1)$$

where h is the building height; the ratio (z/h) represents an idealized linear mode shape; $p(z,t)$ is the horizontal wind load at elevation z ; and M_B is the measured overturning moment.

This assumption soon became an interesting research topic and many studies were conducted to assess its acceptance in the response prediction (Holmes 1987, Boggs 1989, Xu 1993, Yip 1995, Xie 1998, Chen 2005). In these studies, a range of mode shape nonlinearity was considered by assuming idealized gust wind profiles with a range of power law exponents. As a result of these studies, a number of schemes for mode shape corrections were proposed. In general, different mode shape correction factors are needed for different response components.

For a building in a typical urban setting, the wind environment could be much more complicated than that represented by the idealized wind profiles. With aerodynamic interactions and wake effects generated by adjacent structures, the gust wind profile is complex. In some cases, the wind gust at the upper and lower portions of a building can have an opposite phase. Aware of these complications, Xie and Irwin (1998) proposed a new analytical framework that determines the generalized force for nonlinear mode shapes directly, so that the need for gust wind profile assumptions and the mode shape correction factors can be eliminated. The key step of this method is to identify the equivalent gust wind pressure distributions from the simultaneously measured overturning moments and base shears. Although a representative pressure distribution for torsion cannot be identified in the same way as for shears, a rational choice is to assume the pressure distributions for torsion have a similar shape as the weighted pressure distributions of shears. This implies that the exterior torsional loads are induced by the eccentricity of the exterior shears. With this method, the generalized force for the j -th mode is given by

$$\begin{aligned} \tilde{P}_j(t) = & \left(Y_{jF_x} + \Lambda_{jF_x} \right) F_x(t) + \left(Y_{jF_y} + \Lambda_{jF_y} \right) F_y(t) \\ & + \left(Y_{jM_y} + \Lambda_{jM_y} \right) \frac{M_y(t)}{h} + \left(Y_{jM_x} + \Lambda_{jM_x} \right) \frac{M_x(t)}{h} + Y_{jM_z} \frac{M_z(t)}{r} \end{aligned} \quad (2)$$

where F_x and F_y = measured base shears in two orthogonal directions;

M_y and M_x = measured base overturning moments in two orthogonal directions;

M_z = measured base torque;

$Y_{j[l]}$ and $\Lambda_{j[l]}$ = contribution factors as functions of mode shapes and building properties, defined by Xie (1998); and
 r = radius of gyration used for normalizing torsional mode shapes.

1.2 Consideration of structurally-linked buildings

The HFFB method has also been extended to structurally-linked twin buildings or a structurally-linked building complex (Xie and Irwin 1998). For structurally-linked buildings, the differential loading between the buildings is critical for linkage design. To precisely account for the interactions between the building structures, a multi-force-balance (MFB) scheme was developed. MFB measures the exterior wind loads on each substructure (i.e., each building) simultaneously during wind tunnel testing. The generalized forces are then calculated as follows:

$$\tilde{P}_j(t) = \sum_{k=1}^n \tilde{P}_{jk}(t) \quad (3)$$

where the generalized force contributed by the k -th substructure $\tilde{P}_{jk}(t)$ can be determined by Eq. (2). The studies using MFB revealed detailed dynamic interactions between the linked structures and suggested that these interactions could be significant for structural design. Overall, equalization effects between the linked structures are expected. Compared to structurally separated twin buildings, the presence of the structural link between the twin buildings may decrease the response of the building that experiences a higher wind excitation and increase the response of the other building that experiences a lower wind excitation, (Xie and Irwin 2001).

1.3 Consideration of aeroelastic effects

With more super tall buildings being proposed in the recent decade, HFFB encounters new challenges in its applications. Two issues are particularly important. One is the potential for aeroelastic effects and the other is the potential higher-order mode responses. To consider the aeroelastic effects, an aeroelastic model test is normally required. Since an aeroelastic model has to be designed specifically for a set of building dynamic properties, the aeroelastic model tests are typically conducted for the final version of the design and they often serve as a confirmation of the predicted wind response. If the building dynamic properties are further modified after the tests, the aeroelastic model has to be re-modeled and retested to update the wind response. To respond to the practical need for having a good account of aeroelastic effects during structural optimization stages, Xie *et al.* (2007) proposed a new method that includes the aeroelastic effects in the generalized forces. By re-denoting the generalized force shown in Eq. (2) as $\tilde{P}_{jB}(t)$, meaning the buffeting term of the generalized force, the additional aeroelastic term can be introduced, denoted by $\tilde{P}_{jA}(\dot{\delta}_j, \delta_j)$ where $\dot{\delta}_j$ and δ_j are the modal velocities and modal deflections, respectively. Subsequently, the total generalized force can be represented as the linear combination of the two contributions.

$$\tilde{P}_j(t) = \tilde{P}_{jB}(t) + \tilde{P}_{jA}(\dot{\delta}_j, \delta_j) \quad (4)$$

Based on linear aeroelastic theory, the aeroelastic term is expressed by:

$$\tilde{P}_{jA}(\delta_j, \dot{\delta}_j) = \frac{1}{2} \rho U_r^2 B_r h \left[\begin{array}{l} K(H_{1x}(K)C_{xj} + H_{1y}(K)C_{yj} + A_1(K)C_{\theta j}) \frac{\dot{\delta}_j(t)}{U_r} \\ + K^2(H_{2x}(K)C_{xj} + H_{2y}(K)C_{yj} + A_2(K)C_{\theta j}) \frac{\delta_j(t)}{B_r} \end{array} \right] \quad (5)$$

where ρ = air density; U_r = reference wind speed; B_r = reference building width; $K = \frac{\omega B_r}{U_r} =$

reduced frequency; $H_{[j]}$ and $A_{[j]}$ = aeroelastic parameters for sway and torsional motion; and $C_{[j]}$ = coefficients related to mode shapes and building geometry.

The only missing information in the aeroelastic terms, Eq. (5), is the non-dimensional aeroelastic parameters that are the function of the reduced frequency, the building shape, and the wind conditions. The proposed method includes an identification scheme to determine these aeroelastic parameters using a soft-mounted force balance model. The validation of this method is still in process and will not be further discussed in the present paper.

1.4 Comments on pressure integration method

A more versatile wind tunnel method that uses simultaneously measured pressures over the entire building envelope became available in the early 1990s (Irwin and Kochanski 1995). This method, called high-frequency pressure integration (HFPI), allows identification of the detailed wind load distributions and thus it eliminates the shortcomings of the HFFB method. The HFPI method has been used with success in assessing higher-order mode response. For very complicated structures, HFPI was proved to be a better test method than HFFB (Xie and To 2005). However, owing to its simplicity, HFFB continues to be used as a convenient and quick tool for determining wind response. In cases where pressure measurement is difficult to perform, such as for buildings with truss elements or balconies, or in presence of other architectural features on the building surfaces, HFFB is still a primary choice. With newly developed HFFB adopted for aeroelastic model tests (as described in Section 1.3), HFFB has found a new usage in wind engineering studies of buildings, in particularly for building aerodynamic optimization studies.

Since HFPI can measure detailed load distributions, it is an ideal tool for validation of the assumptions used in HFFB technique. It has been found that for most buildings, the HFFB and the HFPI method provide very consistent results.

2. Analytical validation for non-linear mode shapes

This section provides an analytical validation for the method proposed by Xie and Irwin (1998) for analysis of the nonlinear mode shape effects. The validation is conducted for a case where a set of wind profiles is assumed and an uncoupled nonlinear mode shape for a building with the total height h and a uniform building width B is expressed by $\Phi_x = (z/h)^\beta$.

Based on quasi-static buffeting theory, the exterior dynamic wind loads at elevation z are approximated by

$$p(z, t) = \rho U_z u_z(t) B C_F \tag{6}$$

where U_z and u_z are the mean and fluctuating wind speed at elevation z ; and C_F is the force coefficient. By assuming the mean wind speed profile and turbulence intensity profile to be

$$U_z = U_r \left(\frac{z}{h} \right)^{\alpha_M}; \quad I_u(z) = I_r \left(\frac{z}{h} \right)^{-\alpha_T} \tag{7}$$

where α_M and α_T are the specified exponents of mean speed and turbulence intensity profiles, respectively, the power spectrum of the base shear can be calculated

$$S_F(f) = \int_0^h \int_0^h S_p(z_1, z_2, t) dz_1 dz_2 = 4q_r^2 I_r^2 S_u^*(f) \chi(f) J_F \tag{8}$$

where $q_r = 0.5\rho U_r^2 B C_F$;

$S_u^*(f)$ = normalized power spectrum of wind speed;

$\chi(f)$ = aerodynamic admittance function;

$$J_F = \int_0^h \int_0^h \left(\frac{z_1}{h} \right)^\alpha \left(\frac{z_2}{h} \right)^\alpha \exp\left(-c \frac{fh}{U_r} \left| \frac{z_1}{h} - \frac{z_2}{h} \right| \right) dz_1 dz_2; \text{ and}$$

$\alpha = 2\alpha_M - \alpha_T$ represents the gust wind profile and c is a correlation coefficient.

The power spectra of the base moment and the generalized force can be expressed in a similar way

$$S_M(f) = \int_0^h \int_0^h S_p(z_1, z_2, t) z_1 z_2 dz_1 dz_2 = 4q_r^2 h^2 I_r^2 S_u^*(f) \chi(f) J_M \tag{9}$$

$$S_{P_j}(f) = \int_0^h \int_0^h S_p(z_1, z_2, t) \left(\frac{z_1}{h} \right)^\beta \left(\frac{z_2}{h} \right)^\beta dz_1 dz_2 = 4q_r^2 I_r^2 S_u^*(f) \chi(f) J_{P_j} \tag{10}$$

where $J_M = \int_0^h \int_0^h \left(\frac{z_1}{h} \right)^{\alpha+1} \left(\frac{z_2}{h} \right)^{\alpha+1} \exp\left(-c \frac{fh}{U_r} \left| \frac{z_1}{h} - \frac{z_2}{h} \right| \right) dz_1 dz_2$

$$J_{P_j} = \int_0^h \int_0^h \left(\frac{z_1}{h} \right)^{\alpha+\beta} \left(\frac{z_2}{h} \right)^{\alpha+\beta} \exp\left(-c \frac{fh}{U_r} \left| \frac{z_1}{h} - \frac{z_2}{h} \right| \right) dz_1 dz_2$$

The magnitude of the cross-spectrum between the base shear and the base moment can also be calculated

$$|S_{FM}(f)| = \int_0^h \int_0^h S_p(z_1, z_2, t) z_1 dz_1 dz_2 = 4q_r^2 h I_r^2 S_u^*(f) \chi(f) J_{FM} \tag{11}$$

and
$$J_{FM} = \int_0^h \int_0^h \left(\frac{z_1}{h}\right)^{\alpha+1} \left(\frac{z_2}{h}\right)^a \exp\left(-c \frac{fh}{U_r} \left|\frac{z_1}{h} - \frac{z_2}{h}\right|\right) dz_1 dz_2$$

By including the assumed mode shape function and wind profiles shown in Eq. (7) in the calculation of contribution factors, Eq. (2) is simplified

$$\tilde{P}_j(t) = \frac{1}{h(1+\beta)(2+\beta)} \left[2(1-\beta)hF_x(t) + 6\beta M_y(t) \right] \tag{12}$$

and the generalized force spectrum reads as follows

$$S_{P_j^*}(f) = 4q_r^2 I_r^2 S_u^*(f) \chi(f) \left(\frac{1}{(1+\beta)(2+\beta)} \right)^2 \left[4(1-\beta)^2 J_F + 24(1-\beta)\beta J_{FM} + 36\beta^2 J_M \right] \tag{13}$$

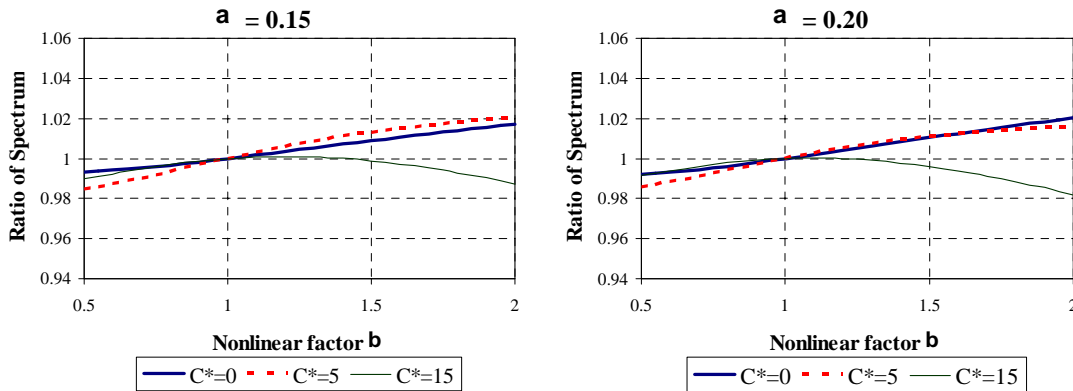


Fig. 1 Spectrum ratio from Eq. (14)

The ratio of the generalized spectrum obtained from Eq. (10) and that of Eq. (13) is a measure of the approximation introduced by using the method proposed by Xie and Irwin for nonlinear mode shapes. This ratio is a function of the wind profile α , nonlinear mode shape factor β , and the vertical correlation parameter $C^* = c(fh/U_R)$ as follows

$$\frac{S_{P_j^*}(f)}{S_{P_j}(f)} = \left(\frac{1}{(1+\beta)(2+\beta)} \right)^2 \left[4(1-\beta)^2 \frac{J_F}{J_{P_j}} + 24(1-\beta)\beta \frac{J_{FM}}{J_{P_j}} + 36\beta^2 \frac{J_M}{J_{P_j}} \right] \tag{14}$$

Fig. 1 shows that the spectrum ratios are all within 2% for a wide range of parameters, indicating that the building response obtained by using Xie and Irwin’s method is close to the theoretical prediction ($< \sqrt{2}\%$). It should be noted that this small difference is caused by the

deviation between the assumed wind pressure profile (i.e., power law profile) and the assumed linear pressure profile. An actual gust pressure profile is more complicated, and there is no evidence showing that a power law profile is generally more precise than a linear profile. In fact, in a heavily built-up urban setting, the gust pressures at a building's bottom portion can be in an opposite phase from those at the building's upper portion. The linear profile is more flexible to represent this situation.

A similar theoretical validation study was also attempted by Chen and Kareem (2005). Unfortunately, due to a mathematical error in deducing Eq. (13) from Eq. (12), incorrect results were presented.

3. Experimental validation by using pressure integration models

The analytical validation as described above is for an ideal building with simple geometry. In engineering practice, the buildings can have geometric features which make analytical validation very difficult. As discussed in Section 1.4, the high-frequency pressure integration (HFPI) method not only provides an alternative wind tunnel approach, but also provides a tool for validating HFFB method.

To use HFPI for HFFB validation, the authors and their colleagues have conducted several experiment studies (Garber *et al.* 2007). In these studies, instead of conducting parallel tests using a pressure model and a HFFB model, only the wind tunnel data from pressure tests were utilized. By simultaneous integration of pressures over the building envelope, two sets of the data were generated: (1) base loads and the generalized forces associated with various modes of vibration, for detailed HFPI analysis, and (2) base loads only for HFFB analysis, as if they had been measured during HFFB tests. In this way, the validations were only focused on the HFFB methodology, and the potential discrepancies from disparity in the data obtained during separate tests were eliminated.

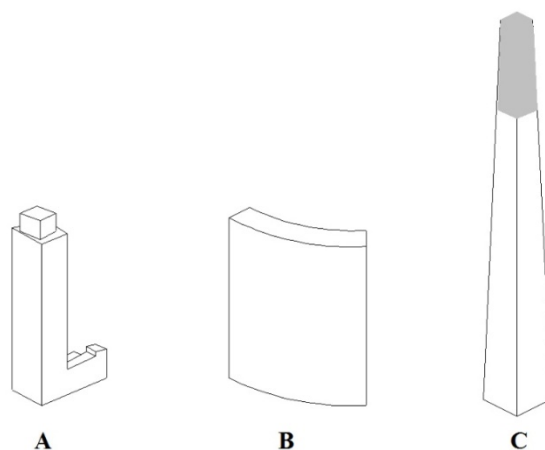


Fig. 2 Illustration of study buildings

Three typical buildings shown in Fig. 2 were selected for the study. Building A represents a typical tall building, except for strong dynamic coupling between the sway motion and rotation. Building B has a wide and curved surface, and also has dynamic coupling between torsion and sway along the narrow face. Building B was thought to be torsionally sensitive, and thus its validation would reveal approximations in prediction of torsional response from HFFB data. Building C has a porous upper portion that is aerodynamically very different from the remainder of the tower.

The HFFB analysis was conducted using the improved HFFB method given by Eq. (2).

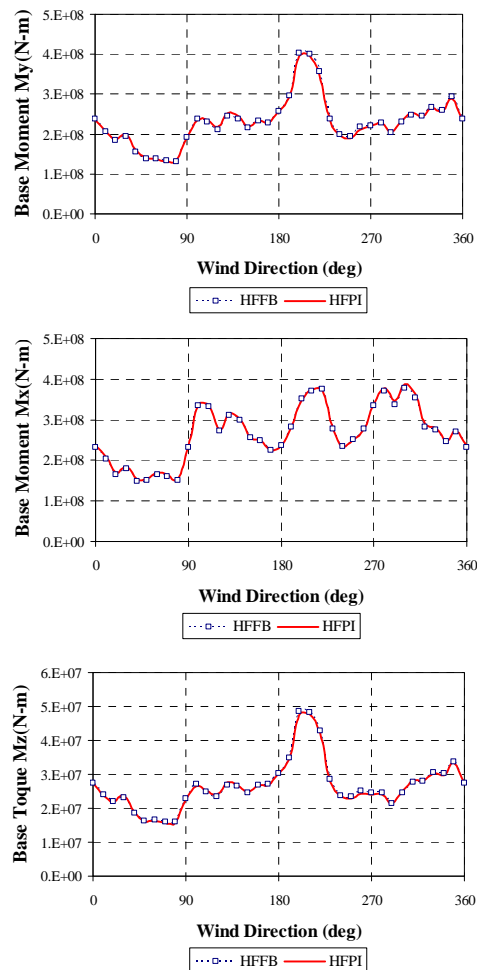


Fig. 3 Inertial components of base overturning moments and torque for Building A

3.1 Validation of overall loads at base

Fig. 3 shows the comparisons of the inertial (resonant) components of the base overturning moments and the base torque for Building A. Good agreements between HFFB and HFPI were observed for all wind directions. The agreement for the base torque can be considered as a confirmation that the dynamic coupling has been handled properly by the HFFB method.

For Building B, while the horizontal loads showed good agreement between HFFB and HFPI, some noticeable differences for the base torque were observed, as depicted in Fig. 4. This is consistent with the common belief that the torsional response predictions using HFFB method involve more approximation than those for the sway response. However, it is important to note that relatively large differences between HFFB and HFPI results were mostly for lower responses. At wind directions with high torsional response, these discrepancies did not exceed 6%. The main assumption included in the HFFB analysis for torsion was that the slope of the equivalent torsional pressure distribution over the building height was the same as the weighted average of the slope for shear forces in two orthogonal directions. This assumption seems to work well for response where torsion is dominant.

Building C presented a new challenge for using HFFB. Since the upper portion and the lower portion of the building had different aerodynamic characteristics, an assumption had to be made about the coefficient ratio of the aerodynamic forces exerted on the two portions, needed to estimate the generalized forces. This ratio was assumed to be equal to the solidity ratio, which seemed reasonable for along-wind loading but could be imprecise for across-wind loading. Fig. 5 shows that the differences between HFFB and HFPI results were mostly for high inertial loading, which was mainly associated with the across-wind response of the building. It should be noted that for porous surfaces, pressure integration measurements also have limitations. An alternative approach with HFFB is to measure the overall loading and, as an extra test, to measure the loading on the porous portion only, by shielding the solid portion of the building. In this way, a more precise ratio of the aerodynamic force coefficients can be obtained, see Fig. 6.

Although differences between inertial loads obtained from the HFFB and HFPI techniques, were noted, they were mainly observed in the estimates of building accelerations. For structural design loading, they were relatively smaller, as a result of including the static load components.

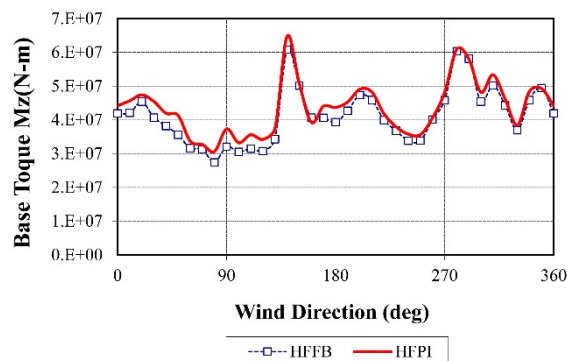


Fig. 4 Inertial base torque of Building B

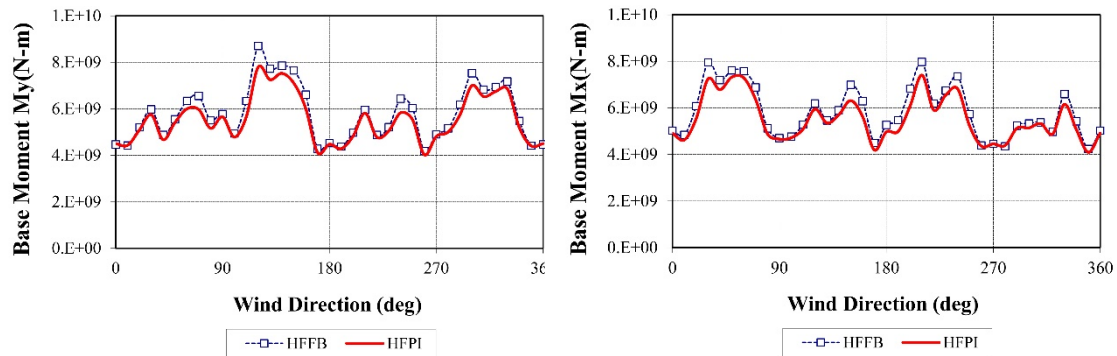


Fig. 5 Inertial components of overturning moments of Build C



Fig. 6 Example of portional HFFB

3.2 Validation of wind load distributions

Another important comparison of the HFFB and HFPI analysis was the load distributions. For the convenience of structural designers, the predicted design wind loads are typically presented as effective static floor-by-floor loads. Certainly, due to their dynamic nature and dependence on wind directions, the possible load distributions can be numerous. However, from a practical point of view, the most useful load distribution is the one that represents an envelope of the cumulative loads at each floor level. While HFPI can examine in detail the load effects at each floor level, as a function of wind speed and wind direction and even predict the maximum load effects at each floor level for a given return period, HFFB has to estimate the maximum cumulative loads at each floor level based on the overall structural response.

In the HFFB study, two approaches were considered for the effective load distributions: inertial-priority (I-priority) and quasi-static-priority (QS-priority). With the inertial-priority approach, the maximum building inertial loads are calculated for the design return period and distributed in accordance with the mass distributions and mode shapes. The differences between the predicted total return period loads and the calculated maximum inertial loads were treated as quasi-static loads. These quasi-static loads were then distributed over the building height based on the ratio of moments and shears and the building geometry in a similar manner as the estimate of equivalent pressure distributions. It was found that for buildings with relatively uniform mass density over the building height, the inertial-priority approach tended to provide reasonable and slightly conservative distributions in terms of cumulative load effects. Figs. 7 and 8 give the comparisons of the cumulative loads of Building A and Building B determined from HFPI study and from HFFB using inertial-priority approach.

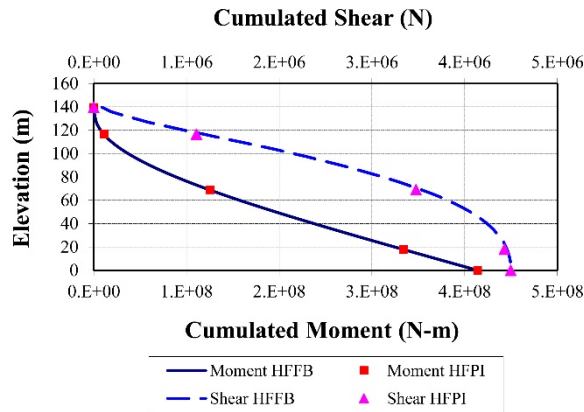


Fig. 7 Cumulative bending moment and shear of Building A

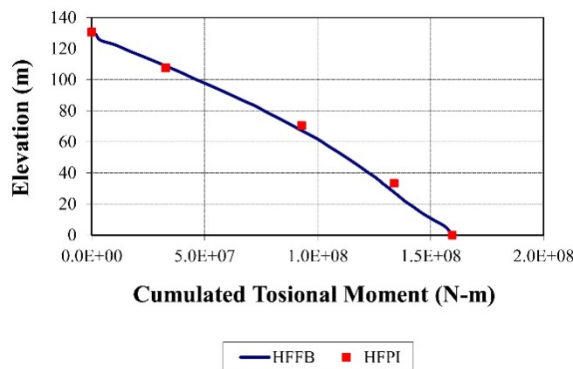


Fig. 8 Cumulative torque of Building B

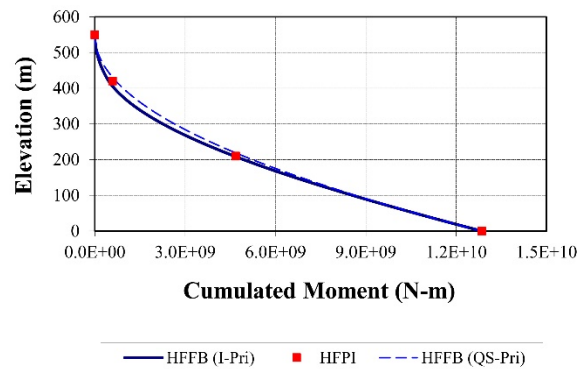


Fig. 9 Cumulative bending moment of Building C

For a building that is significantly lighter at the top, such as Building C, the inertial-priority approach may not be applicable. While the overall wind loads of Building C were dominated by inertial loads of across-wind response, the maximum wind loads on the upper portion were governed by along-wind response. Therefore, the maximum cumulative loads over the building height occurred at different wind directions. With the QS-priority approach, the maximum quasi-static loads were distributed first. Then the inertial loads were applied as the remainder to match the total return-period loads. Fig. 9 indicates that these two approaches likely provide a boundary estimate on the maximum cumulative load distributions.

4. Comparison with field measurements

A 420 m tall, 88-storey office tower, located in Hong Kong, is very close to the seashore in an active typhoon generating area. At the design stage of this building, detailed wind tunnel studies were carried out at RWDI to evaluate its wind-induced responses. The wind tunnel testing included a 1:3000 scale topographic model to determine the local wind conditions at the building site. The information obtained from these tests was then used in the boundary layer wind simulations at the 1:400 scale for high-frequency force-balance (HFFB) model tests. The predicted wind-induced building responses, including the design wind loads and building accelerations, were then incorporated in the structural design of the building.

To investigate the building's wind-induced responses at full-scale and to verify the wind tunnel predictions, City University of Hong Kong installed a wind and building vibration monitoring system, including anemometers, accelerometers, GPS and pressure sensors on the building and successfully measured the building responses during the passages of several typhoons in 2007 and 2008. The building dynamic properties were also identified from the measurements.

Based on the measured dynamic properties, the wind-induced building responses were re-calculated using the HFFB model data obtained at the design stage of the building. Comparisons were then made between the field-measured accelerations and those from the wind tunnel testing to evaluate the accuracy of the HFFB technique used in the wind tunnel tests (Li *et al.* 2009).

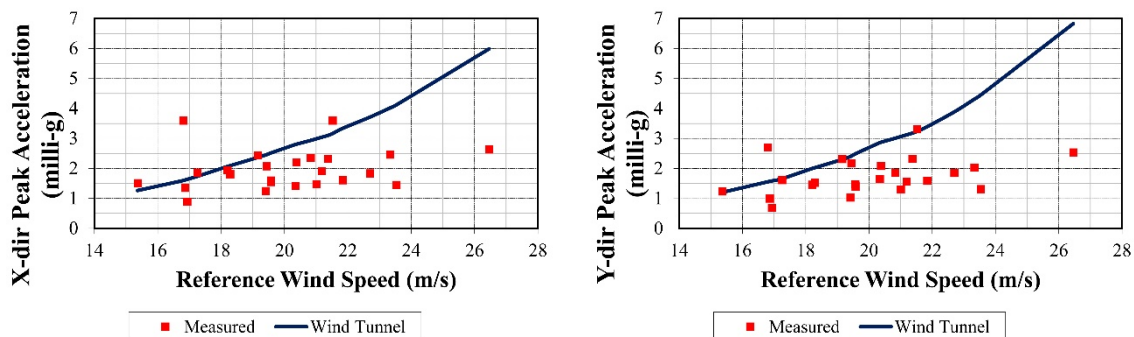


Fig. 10 Comparison between full scale measurements and wind tunnel predictions

The comparison of the wind tunnel results with the full-scale measurements shown in Fig.10 indicates that although considerable scatters exist in the measured data, the accelerations predicted by HFFB method meet practical expectations that the wind tunnel results should represent an envelope of peak responses for the fundamental modal responses. If the higher order modal responses are considered, the total accelerations would be increased by about 6%, which is in a common range of magnitude for higher order mode effects identified by RWDI for similar super-tall buildings using high-frequency pressure integration method and multi-degree aeroelastic model (Xie 2008).

5. Conclusions

A review of the development and improvement of the high-frequency force-balance (HFFB) technique is presented in this paper. Nonlinear mode shape corrections, multi-force balance measurements, and use of a HFFB model to identify aeroelastic parameters are discussed.

For simple building shapes, an analytical validation is discussed for the method to deal with nonlinear mode shapes proposed by Xie and Irwin. The results confirmed that the method offers a simple and flexible tool to account for the nonlinear mode shape effects with negligible deviations from the theoretical values.

For more complicated buildings, high-frequency pressure-integration (HFPI) model studies were used to validate the HFFB method. For a typical tall building with dynamically coupled modes, the HFFB shows a very good agreement with HFPI. For a torsionally sensitive building, HFFB not only provides good estimates on sway response, but also reasonable estimates of torsional response. The assumption that a torsional pressure distribution is similar to the shear pressure distribution seems acceptable. For a building with a porous top, the HFFB analysis is affected by the uncertainties in the aerodynamic characteristics over the building height. In such a case, a portional HFFB test may be conducted to provide refined information on the localized aerodynamic loading.

A comparative study of the wind tunnel predictions and the full-scale measurements was carried out for a super-tall building. It was found that the measured full-scale accelerations were consistent with those obtained from the HFFB model tests. This agreement provides further

evidence that the HFFB wind tunnel tests can lead to reasonably accurate predictions of the wind-induced vibrations of super-tall buildings under typhoon winds.

References

- Boggs, D.W. and Peterka, J.A. (1989), "Aerodynamic model tests of tall buildings", *J. Eng. Mech.- ASCE*, **115**(3), 618-635.
- Boggs, D.W. (1992), "Validation of the aerodynamic model method", *J. Wind Eng. Ind. Aerod.*, **41-44**, 1011-1022.
- Chen, X. and Kareem, A. (2005), "Validity of wind load distribution based on high frequency force balance measurements", *J. Struct. Eng. - ASCE*, **131**(6), 984-987.
- Chen, X. and Kareem, A. (2005), "Dynamic wind effects with coupled modes: application of high frequency force balance measurements", *J. Eng. Mech. - ASCE*, **131**, 1115-1125.
- Garber, J., Browne, M.T.L., Xie, J. and Kumar, K.S. (2007), "Benefits of the pressure integration technique", *Proceedings of the 12th Int. Conf. on Wind Eng.*, Cairns, Australia.
- Holmes, J.D. (1987), "Mode shape corrections for dynamic response to wind", *Eng. Struct.*, **9**, 210-212.
- Holmes, J.D., Rofail, A. and Aurelius, L. (2003), "High-frequency base balance methodologies for tall buildings with torsional and coupled resonant modes", *Proceedings of the 11th Int. Conf. on Wind Eng.*, Lubbock, Texas, USA.
- Irwin, P.A. and Xie, J. (1993), "Wind loading and serviceability of tall buildings in tropical cyclone regions", *Proceedings of the 3rd Asia-Pacific Symp. on Wind Eng.*, Univ. of Hong Kong.
- Irwin, P.A. and Kochanski, W.W. (1995), "Measurement of structural wind loads using the high frequency pressure integration method", *Proceedings of the ASCE Structures Congress, Boston*.
- Li, Q.S., Xie, J., To, A. and Zhi, L.H. (2009), "Wind tunnel studies and their validations with field measurements for a super-tall building", *Proceedings of the 7th Asia-Pacific Conf. on Wind Eng.*, Taipei, Taiwan.
- Tschanz, T. (1982), "The base balance technique for the determination of dynamic wind loads", *J. Wind Eng. Ind. Aerod.*, **13**, 429-439.
- Xie, J. and Irwin, P.A. (1998), "Application of the force balance technique to a building complex", *J. Wind Eng. Ind. Aerod.*, **77-78**, 579- 590.
- Xie, J. and Irwin, P.A. (2001), "Wind-induced response of a twin-tower structure", *Wind Struct.*, **4**(6), 495-504.
- Xie, J. and To, A. (2005), "Design-orientated wind engineering studies for CCTV new building", *Proceedings of the 6th Asia-Pacific Conf. on Wind Eng.*, Seoul, Korea.
- Xie, J., Haskett, T., Kala, S. and Irwin, P.A. (2007), "Review of rigid model studies and their further improvements", *Proceedings of the 12th Int. Conf. on Wind Eng.*, Cairns, Australia.
- Xie, J. (2008), "Progress of wind tunnel techniques in practical applications", *Proceedings of the 4th International Conference on Advances in Wind and Structures (AWAS'08)*, Jeju, Korea

Nomenclature

$A_{[j]}$	aeroelastic parameters for torsional motion
B, B_r	reference building width
c	spatial correlation coefficient of fluctuating wind pressures
$C^* = c(fh/U_r)$	vertical correlation parameter
$C_{[j]}$	coefficients related to mode shapes and building geometry
C_F	force coefficient
F_x, F_y	measured base shears in two orthogonal directions
h	building height
$H_{[j]}$	aeroelastic parameters for sway motion
I_u	wind turbulence intensity
K	reduced frequency;
M_B	measured base moment.
M_y, M_x	measured base overturning moments in two orthogonal directions
M_z	measured base torque
$p(z,t)$	horizontal wind loads at elevation z
$\tilde{P}_j(t)$	generalized force of the j -th mode
r	typical radius of gyration
U_z, u_z	mean and fluctuating wind speed at elevation z
U_r	reference mean wind speed at elevation h
z	vertical elevation
α, α_M	mean wind speed profile
α_T	wind turbulence intensity profile
β	nonlinear mode shape factor
$\dot{\delta}_j, \delta_j$	the j -th modal velocity and deflection
ρ	air density
$Y_{j[l]}, \Lambda_{j[l]}$	contribution factors to the j -th modal force as a function of mode shapes and building properties